Synthesis and Electrorheological Characterization of Polyaniline/Barium Titanate Hybrid Suspension

*Fei Fei Fang, Ji Hye Kim, Hyoung Jin Choi**

Summary: As organic/inorganic composites having attracted much attention due to their heterogeneous physical properties, conducting polyaniline (PANI) and barium titanate ($BaTiO_3$) which possesses large electronic resistance and excellent dielectric strength, were utilized to synthesize PANI/$BaTiO_3$ hybrid which is applicable for an electrorheological (ER) material via 'in-situ' oxidative polymerization. Physical properties of the obtained PANI/$BaTiO_3$ composites were characterized via Fourier-transform infrared spectra (FT-IR), thermogravimetry analysis (TGA), and scanning electron microscopy (SEM). The ER behaviors were investigated via a rotational rheometer, and their shear stresses were fitted using our previously proposed rheological equation of state.

Keywords: barium titanate; electrorheological fluid; polyaniline; shear stress

Introduction

Electrorheological (ER) fluids, a kind of fascinating smart and intelligent materials, are typically composed of colloid particles dispersed in an insulated liquid. They show dramatic, rapid and reversible changes of rheological properties altered by an applied external electric field. Shear viscosity as well as shear stress of the ER fluids are increased abruptly by several orders of magnitude under an electric field. When the electric field is turned on in general, a rapid particle chain formation occurs, by inducing dipoles of the particles aligned along the direction of the applied electric field. If the electric field is maintained, the chains tend to consolidate slowly into thicker columns. Columns of monodisperse particles can eventually organize into a dense phase with body-centered tetragonal symmetry, [1,2] of which the dipoles attract each other in the head-to-tail direction, consequently forming the fibrous aggregates leading to a solid-like state. Thus, in order to make this consolidated fluid flow, we require a force to break these aggregates that comes to the yield stress.[3]

Thereby, ER fluids have stimulated numerous researchers to focus on designing the ER devices such as clutches, brakes, damper, engine mounts and control valves. [4,5] Despite various research and development efforts, these ER devices are still in the early stages of commercialization due to several unsolved problems such as colloidal instability and insufficient amount of yield stress. Researchers have made many efforts to explore various promising materials based on ER fluids which include discussion of inorganic and semi-conducting polymeric particles such as zeolite,[6] carbonaceous particles,[7] conducting PANI,[8] and core-shell composite particulates.[9–12]

Recently, conducting PANI/inorganic composites have attracted much attention due to their heterogeneous physical properties, unique structure and combined merits of the two phases.[13,14] The ER effect of the electroresponsive particles could be enhanced by their modification of the surface over-layer with highly polarizable semiconducting polymer. Therefore, in this study, we synthesized PANI/$BaTiO_3$ composite via

Department of Polymer Science and Engineering, Inha University, Incheon 402-751, Korea
Tel: (+82) 32-860-7486
E-mail: hjchoi@inha.ac.kr

in-situ polymerization. With ferroelectric properties and high dielectric constant as well as good crystallinity of barium titanate, we hope that the obtained PANI/$BaTiO_3$ composite could be suitable for the ER fluid with better ER performance.

Experimental

PANI/$BaTiO_3$ composite was synthesized by an ''in-situ'' polymerization in the presence of hydrophobic $BaTiO_3$ (Inframat Advanced Materials, LLC, USA). First, $BaTiO_3$ nanoparticles with an average size of 100 nm were dispersed in 450 ml of 1 M HCl (Deajung, Korea) to get a homogenous phase by vigorous stirring (200 rpm) at 0 °C, after that aniline monomer was added to this dispersion. Pre-chilled ammonium peroxysulfate (APS) (initiator) which was dissolved in 350 ml of 1 M HCl in another beaker at 0 °C was dropped into separately prepared dispersing phase within 4 h. After dropping the initiator, the mixture was kept stirring at 200 rpm at 0 °C for 24 h. The PANI/$BaTiO_3$ composites were centrifuged, filtered and washed with distilled water, acetone, and methanol to remove excess initiator, monomer, and oligomer, and dried at 65 °C in vacuum oven for 2 days[15].

FT-IR spectroscopy (Perkin Elmer System 2000) was used to identify the chemical structure of the composite prepared by grinding with KBr. Thermal stability of both PANI and PANI/$BaTiO_3$ composite were examined by using a thermogravimetric analyzer (TGA, TA instrument Q50, USA). XRD spectra was performed via a Rigaku DMAX 2500 ($\lambda = 1.54$ Å) diffractometer. Scanning electron microscopy (SEM, S-4300, Hitachi) was utilized to observe the morphology of the obtained samples. Electrical conductivity was measured by a standard 2-probe method using a picoameter at room temperature.

In order to apply the composite for an ER fluid, we have to control the conductivity of the obtained PANI/$BaTiO_3$ composite by a dedoping process. We dispersed the composite in 1 M NaOH solution and monitored the pH at 9 by dropping either 1 M NaOH or 1M HCl solution.[16] The dedoped sample was then filtered, dried, and sieved. The conductivity was found to be decreased from 2.41×10^{-1} to 1.67×10^{-12} S/cm. Finally the PANI/$BaTiO_3$ composite was dispersed in silicone oil (kinematic viscosity: 50cS, density: 0.96 g/ml) to prepare a 10 vol% ER fluid. ER behaviors were investigated by a rotational rheometer (Physica MC 120, Stuttgart) equipped with a DC high voltage generator. In order to get a valid experimental result, we repeated every experiment at 25 °C for 3 times.

Results and Discussion

In order to confirm the chemical structures, FT-IR spectra of synthesized PANI, $BaTiO_3$, and PANI/$BaTiO_3$ composite were taken, and it was found that the characteristic peaks of the PANI appeared at about 1593 cm^{-1}, 1498 cm^{-1}, 1308 cm^{-1} and 832 cm^{-1} were attributed to quinone ring deformation, benzene ring deformation, C–N stretch of aromatic amine and aromatic C–H out of plane, respectively. Distinctive peak of $BaTiO_3$ detected at about 568 cm^{-1} and 438 cm^{-1} were appointed to Ti–O band and Ti–O bending vibrations. [17]

TGA curves given in Fig. 1 demonstrate not only the content of $BaTiO_3$ in the composite but also the change in thermal stability between pure PANI and PANI/$BaTiO_3$ composite. TGA test was carried out under air with a heating rate of 20 °C/min. The onset decomposition temperature of PANI/$BaTiO_3$ composite was higher than that of pure PANI. This behavior confirmed the enhanced thermal stability due to the retardation effect of inorganic material on the decomposition of the composite. Residual weight of the PANI/$BaTiO_3$ composite was also found to be dependent on the content of $BaTiO_3$ nanoparticles. In this composite, $BaTiO_3$ content was approximately 25 wt%.

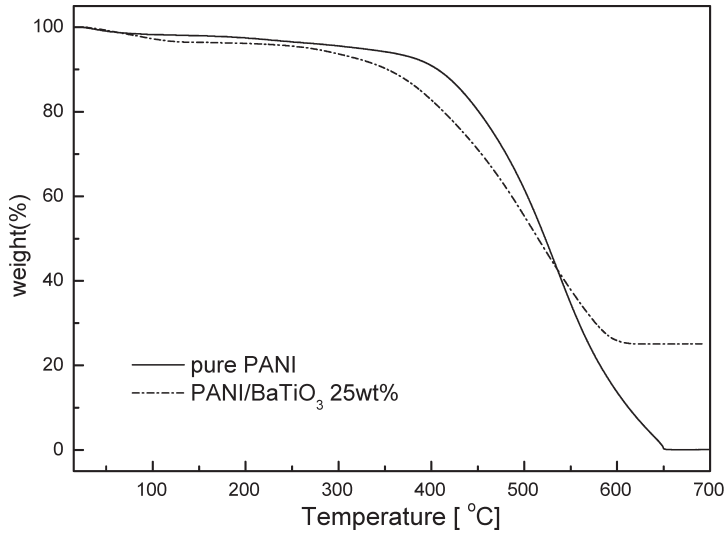

Figure 1.
TGA curves of pure PANI (solid line) and PANI/$BaTiO_3$ composite (dashed line).

X-ray diffraction patterns of the PANI, $BaTiO_3$ nanoparticles and PANI/$BaTiO_3$ composite were indicated in Figure 2. Figure 2(a) shows a typically wide amorphous peak for pure PANI at low 2θ region. Figure 2(c) represents that $BaTiO_3$ possessed good crystallinity. When $BaTiO_3$ nanoparticles were embedded into the polymer matrix, the interaction between PANI and $BaTiO_3$ restricted the growth of PANI chains around $BaTiO_3$ nanoparticles and influenced the crystallinity of the

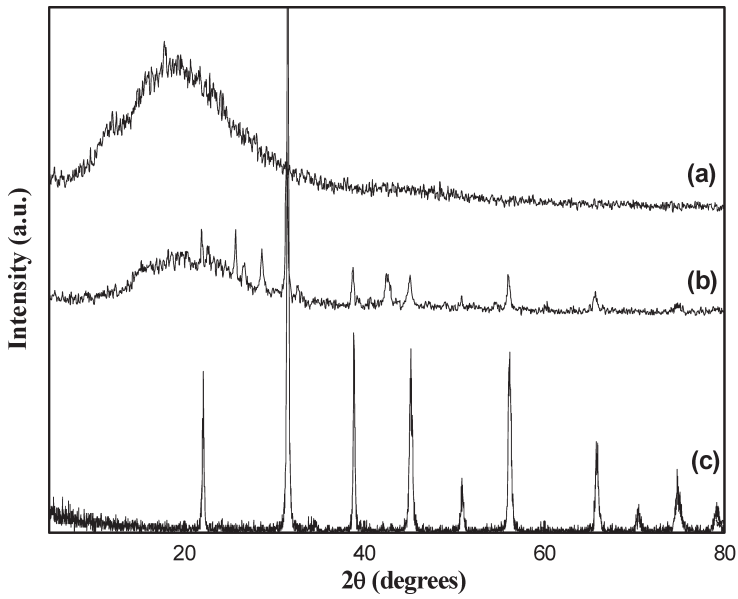

Figure 2.
XRD spectra of (a) PANI, (b) PANI/$BaTiO_3$ composite, and (c) $BaTiO_3$.

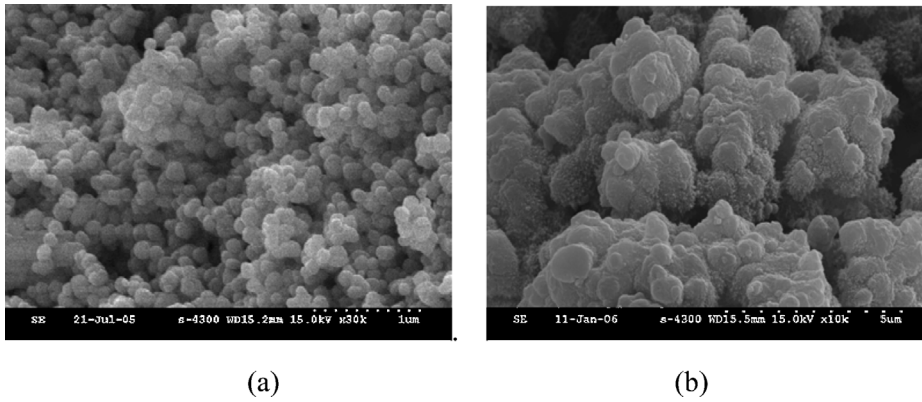

Figure 3.
SEM images of $BaTiO_3$ nanoparticles (a) and PANI/$BaTiO_3$ composite (b).

inorganic $BaTiO_3$ leading to a decreased peak density as shown in Fig. 2(b). In addition, the broad peak attributed to polymer appeared in Fig. 2(b) showed the successful deposit of PANI on the surface of $BaTiO_3$ nanoparticles.

By comparing the SEM images of Figs. 3(a) and 3(b), we found that the size of the spherical particles was increased distinctively which may be interpreted by the embedding of inorganic $BaTiO_3$ particles into the PANI polymeric matrix. $BaTiO_3$ possessed a nearly spherical morphology with an average size around 100 nm, while the PANI had a planar appearance due to its intrinsic rigid molecular structure.[18]

Figure 4 shows that the PANI/$BaTiO_3$ composite based ER fluid implies very typical ER performance. It behaved like a

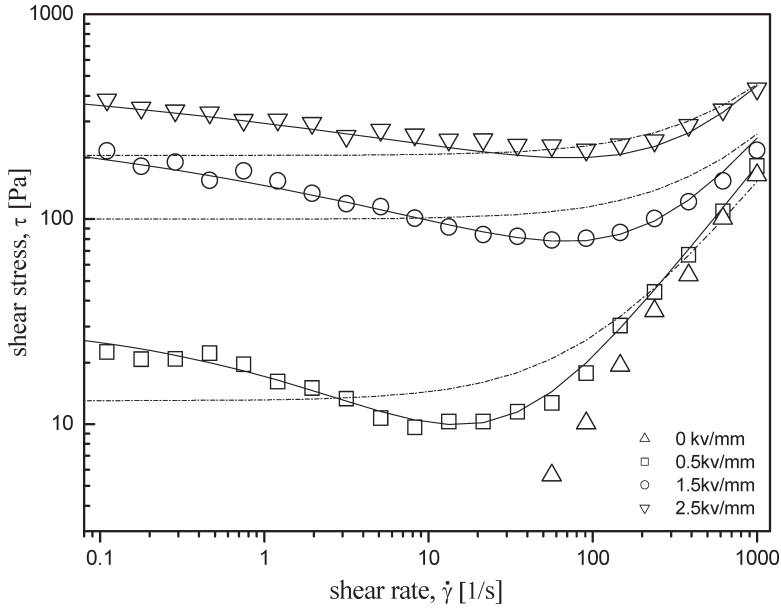

Figure 4.
Fit of model equations to flow curves for PANI/$BaTiO_3$ composite based ER fluids with three different electric field strengths. Dashed line is for Bingham model (Eq. (1)), solid line for our suggested model (Eq. (2)).

Newtonian fluid without an external electric field, in which the shear stress increases linearly with a shear rate. Meanwhile under an electric field, the ER fluid showed a Bingham-like behavior because the particles got polarized and formed chain-like structures. The plateau region of shear stress for a wide range of shear rates under an applied electric field could be explained by the reformation of the broken chain like structure. By increasing the electric field strength, the shear stress abruptly increased over the entire shear rate range. This behavior has also been observed for various semiconducting polymer-based ER fluids.[19–21] We obtained relatively high shear stress tested at 2.5 kV/mm compared with that from the previous study.[22]

On the other hand, it is well known that the yield stress is one of the critical design parameters in the ER phenomenon and has attracted considerable attention both experimentally and theoretically. Among those discoveries, the Bingham equation has been frequently quoted to describe the shear stress behavior with a non-vanishing yield stress (τ_y), which is defined as a stress where the suspension changes from solid-like to fluid-like at a zero shear rate limit [23]. This simplest model with two parameters is given below:

$$\begin{array}{ll} \tau = \tau_y + \eta\dot{\gamma} & \tau \geq \tau_y \\ \dot{\gamma} = 0 & \tau < \tau_y \end{array} \qquad (1)$$

Here, τ_y is a function of an electric field, $\dot{\gamma}$ is the shear rate, and η is the shear viscosity. However, after more and more ER fluids were developed, the Bingham model was found to be not enough to give an all-side information about the shear stress behavior because the shear stress often gives complicated behaviors.[24] Thereby, extensive researches on quantitative analysis to describe both yield stress and shear stress behaviors became prevailing,[25–27] but only a few reports on the constitutive equation were found because many reported constitutive equations are too complicated to be used. Therefore, a model constitutive rheological equation of state was suggested [28,29] to analyze the ER fluids under an applied electric field more comprehensively instead of their quantitative interpretation as follows;

$$\tau = \frac{\tau_y}{1 + (t_2\dot{\gamma})^{\alpha}} + \eta_\infty \left(1 + \frac{1}{(t_3\dot{\gamma})^{\beta}}\right)\dot{\gamma} \qquad (2)$$

The first term of the right-hand sides in Eq. (2) implies the shear stress behavior at a low shear rate region especially in the case of the decrease of shear stress and the second term describes well the shear stress behavior at a high shear rate region. Here, α is related to the decrease in the shear stress, t_2 and t_3 are time constants, and η_∞ is the shear viscosity at a high shear rate and is interpreted as the shear viscosity in the absence of an electric field. The exponent β has the range $0 < \beta \leq 1$, since $d\tau/d\dot{\gamma} \geq 0$. The fitting of the model equation to flow curve for PANI/$BaTiO_3$ composite based ER fluids were shown in Fig. 4. It is clear that the solid lines originated from the suggested constitutive equation model of Eq. (2) fitted the flow curve data very accurately through the whole shear range, especially the data investigated at relative low shear rate region. Compared with our model, the Bingham model given in Eq. (1) was not enough to describe the data comprehensively. Furthermore, it was found that the yield stresses obtained from the Bingham fluid model are much lower than that from our model. This can be explained from the fact that our proposed model accurately fits the decrease in the shear stress for the region of shear rate from 0 to 100 (1/s), while Bingham model does not fit the data accurately. The large deviation between two models is observed especially at the low shear rate.

Conclusion

PANI/$BaTiO_3$ composite was synthesized via an in-situ oxidative polymerization. Both FT-IR spectra and SEM images helped to give some informations on the chemical formation and the morphology of the obtained PANI/$BaTiO_3$ composite

separately. The thermal stability of the PANI/$BaTiO_3$ composite was increased compared with that of the PANI due to the embedding of the inorganic particles in the polymer matrix. PANI/$BaTiO_3$ composite based ER fluid gave typical ER behaviors, showing higher shear stress than that of pure PANI which was attributed to the influence of $BaTiO_3$ nanoparticles on the conducting PANI due to its high dielectric performance. We also employed a suggested constitutive equation to fit the shear stress and it was found to be more accurate compared with the traditional Bingham equation.

Acknowledgement: This work was supported by National Research Laboratory (NRL) Program in Korea (2006).

[1] T. J. Chen, R. N. Zitter, R. Tao, *Phys. Rev. Lett.* **1992**, 68, 2555.
[2] R. Tao, *Phy. Rev. E* **1993**, 47, 423.
[3] Y. D. Kim, D. De Kee, *AIChe J.* **2006**, 52, 2350.
[4] G. Bossis, C. Abbo, S. Cutillas, S. Lacis, C. Métayer, *Int. J. Mod. Phys. B* **2001**, 15, 564.
[5] J. W. Kim, C. A. Kim, H. J. Choi, S. B. Choi, *Korea-Australia Rheol. J.* **2006**, 18, 25.
[6] J. C. Ryu, J. W. Kim, H. J. Choi, S. B. Choi, J. H. Kim, M. S. Jhon, *J. Mater. Sci. Lett.* **2003**, 22, 807.
[7] A. Bezryadin, R. Westervelt, M. Tinkham, *Phys. Rev. E* **1999**, 59, 6896.
[8] V. Pavlinek, P. Saha, J. Perez-Gonzalez, L. De Vagras, J. Stejskal, O. Quadrat, *Appl. Rheol.* **2006**, 16, 14.
[9] O. Quadrat, J. Stejskal, *J. Ind. Eng. Chem.* **2006**, 12, 352.
[10] N. Kohut-Svelko, S. Reynaud, R. Dedryvère, H. Martinez, D. Gonbeau, J. Francois, *Langmuir* **2005**, 21, 1575.
[11] X. P. Zhao, J. B. Yin, *J. Ind. Eng. Chem.* **2006**, 12, 184.
[12] J. B. Jun, J. W. Kim, K. D. Suh, *Macromol. Chem. Phys.* **2002**, 203, 1011.
[13] C. Sanchez, G. J. A. A. Soler-Illia, F. Ribot, T. Lalot, C. R. Mayer, V. Cabuil, *Chem. Mater.* **2001**, 13, 3061.
[14] J. H. Wei, J. Shi, J. G. Guan, R. Z. Yuan, J . *Mater. Sci.* **2004**, 39, 3457.
[15] A. Maity, M. Biswas, *J. Ind. Eng. Chem.* **2006**, 12, 311.
[16] E. V. Strounina, R. Shepherd, L. A. P. Kane-Maguire, G. G. Wallace, Synth . *Met.* **2003**, 135–136, 289.
[17] H. Reverón, C. Aymonier, A. Loppinet-Serani, C. Elissalde, M. Maglione, F. Cansell, *Nanotechnology* **2005**, 16, 1137.
[18] I. S. Lee, J. Y. Lee, J. H. Sung, H. J. Choi, *Synth. Met.* **2005**, 152, 173.
[19] P. Dong, C. Wang, S. Zhao, *Fuel* **2005**, 84, 685.
[20] J. H. Kim, F. F. Fang, K. H. Lee, H. J. Choi, *Korea-Australia Rheol. J.* **2006**, 18, 103.
[21] J. H. Sung, D. P. Park, B. J. Park, H. J. Choi, *J. Ind. Eng. Chem.* **2006**, 12, 301.
[22] J. H. Sung, I. S. Lee, H. J. Choi, *Int. J. Mod. Phys. B* **2004**, 19, 1128.
[23] L. Xiang, X. P. Zhao, *J. Colloid Interf. Sci.* **2006**, 296, 131.
[24] S. J. Park, M. S. Cho, S. T. Lim, H. J. Choi, M. S. Jhon, *Macromol. Rapid Commun.* **2005**, 26, 1563.
[25] H. See, *J. Phys. D: Appl. Phys.* **2000**, 33, 1625.
[26] X. Duan, H. Chen, Y. He, W. Luo, *J. Phys. D: Appl. Phys.* **2000**, 33, 696.
[27] P. O. Brunn, B. Abu-Jdavil, *Rheol. Acta* **2004**, 43, 62.
[28] M. S. Cho, H. J. Choi, M. S. Jhon, *Polymer* **2005**, 46, 11484.
[29] C. H. Hong, H. J. Choi, M. S. Jhon, *Chem. Mater.* **2006**, 18, 2771.

